NASA Contractor Report 181793

Performance of the Active Sidewall Boundary-Layer Removal System for the Langley 0.3-Meter Transonic Cryogenic Tunnel

S. Balakrishna, W. Allen Kilgore, and A. V. Murthy

Vigyan Research Associates, Inc.
Hampton, VA 23665-1325

February 1989

National Aeronautics and Space Administration

Langley Research Center
Hampton, Virginia 23665

SUMMARY

A performance of an active sidewall boundary-layer removal system for the Langley 0.3-m Transonic Cryogenic Tunnel (TCT) was evaluated in 1988. This system uses a compressor and two throttling digital valves to control the boundary-layer mass flow removal from the tunnel. The compressor operates near the maximum pressure ratio for all conditions. The system uses a surge prevention and flow recirculation scheme. A microprocessor based controller is used to provide the necessary mass flow and compressor pressure ratio control. Initial tests on the system indicated problems in realizing smooth mass flow control while running the compressor at high speed and high pressure ratios. An alternative method has been conceived to realize boundary-layer mass flow control which avoids the recirculation of the compressor mass flow and operation near the compressor surge point. This scheme is based on varying the speed of the compressor for a sufficient pressure ratio to provide needed mass flow removal. The system has a mass flow removal capability of about 10% of test section flow at M=0.3 and 4% at M=0.8. The system performance has been evaluated in the form of the compressor map, and compressor tunnel interface characteristic covering most of the 0.3-m TCT operational envelope. A simple analytical model which describes the compressor-tunnel interface flow mechanics has been proposed and validated.

INTRODUCTION

It is well known that airfoil aerodynamic data obtained from two-dimensional wind tunnels are affected by wall interference. At transonic speeds the wall interference can be significant. Studies at the 0.3-m TCT aim to minimize the wall interference on airfoil measurements using such concepts as flexible wall adaptation for top and bottom walls and sidewall boundary-layer treatment schemes. The sidewall boundary-layer treatment is known to reduce the test section boundary-layer thickness thereby reducing the possibility of flow separation on the sidewall and at the model. (ref. 1)

At the 0.3-m TCT, a sidewall boundary-layer removal system has been used in a phased manner during 1980-88. Since the 0.3-m TCT is a closed circuit pressure tunnel, removing mass flow from the sidewalls by discharging the flow to the atmosphere is feasible whenever the static pressure of the test section is higher than ambient pressure. In this passive discharge scheme, the amount of mass flow that can be removed is limited to the mass flow of liquid nitrogen (LN_2) being injected into the tunnel to maintain the tunnel testing conditions. A first phase study, during 1981, established the limits of the performance of the passive boundary-layer removal scheme. (ref. 2) It pointed to the need for higher mass flow removal rates for full control of boundary-layer and flow separation in the test section. Higher rates of removal results in a mass enthalpy unbalance to the tunnel leading to total

loss of tunnel control. Many schemes for obtaining a higher mass flow removal capability were considered for the 0.3-m TCT. (ref. 3) Amongst these, an active sidewall boundary-layer removal scheme was chosen to be used with the 0.3-m TCT. In this scheme, a compressor removes mass from the sidewall boundary-layer in the test section and reinjects the mass back into the tunnel at the downstream diffuser. The tunnel is not upset by a mass unbalance since there is no net mass loss from the tunnel circuit. However, the tunnel thermal equilibrium is disturbed by the compressor induced temperature rise of the mass. This compressor energy coming into the tunnel circuit can be cancelled by injecting extra LN_2 at an appropriate point.

An electrical motor driven centrifugal compressor capable of pressure ratio of about 2.4 at a mass flow of 8 kg/s was chosen for the active sidewall boundary-layer removal scheme. In 1984, the limits of performance for this compressor system were evaluated experimentally. (ref. 4) Based on this evaluation, the control scheme for sidewall boundary-layer removal was finalized. The controller scheme requires operating the compressor at a high speed and fixed pressure ratio with a surge prevention and flow recirculation capability, and for LN_2 injection at the compressor inlet to cancel the compressor induced heat.

A microprocessor based controller has been designed to provide mass flow control, temperature control, and surge protection as defined by the controller scheme. The sidewall boundary-layer removal system with its microprocessor based controller, flow path control, compressor speed control and the measuring system were put through a performance evaluation during 1988. The results of the system evaluation are presented in this paper.

SYMBOLS

Nomenclature:

A	area, m^2
A_d	tunnel cross sectional area at compressor flow reinjection point in diffuser, m^2
A_t	test section area, m^2
A_v	valve area, normalized to unity when full open and zero at full close
C_D	digital valve pressure drop coefficient
C_{D1}	flow coefficient
K	test section mass flow constant
k	gas constant
k_1	valve pressure drop constant
k_2	inlet line drop constant (function of k, k_1 and A_t)

M	test section Mach number
M_d	flow Mach number at compressor flow reinjection point in diffuser
$\dot{m}$	mass flow rate, kg/s
$\dot{m}_{bl}$	total boundary-layer removal mass flow rate, kg/s
$\dot{m}_t$	test section mass flow rate, kg/s
N	compressor motor speed, rpm
P	pressure, psia
P_d	total pressure at compressor flow reinjection point in diffuser, psia
P_{in}	compressor inlet pressure, psia
P_{out}	compressor outlet pressure in the reinjection duct near tunnel, psia
P_s	test section static pressure, psia
P_{sd}	static pressure at compressor flow reinjection point in diffuser, psia
P_t	tunnel total pressure, psia
ΔP	pressure drop across digital valve, psia
R	compressor pressure ratio, P_{out}/P_{in}
T	tunnel total temperature, K
ΔT	temperature rise across the compressor, K
v	velocity, m/s
Z	compressibility factor
α	percentile ratio of mass flows, $100(\dot{m}_{bl}/\dot{m}_t)$
ρ	density of tunnel gas, kg/m^3
γ	ratio of specific heats, C_p/C_v

Units:

HP	horsepower
Hz	Hertz
kg	kilograms
K	kelvin
KW	kilowatt
m	meter
psia	pounds per square inch (absolute)
rpm	revolutions per minute
s	second

DESCRIPTION OF 0.3-m TCT AND SIDEWALL BOUNDARY- LAYER REMOVAL SYSTEM

The Langley 0.3-m TCT can test airfoil models at flight equivalent Reynolds numbers over a wide range of speeds. It is a closed-circuit continuous flow pressure-tunnel which uses cryogenic nitrogen as the test gas. (ref. 5) The tunnel aluminum pressure shell is externally insulated to prevent heat gains. The tunnel has a 13 x 13 inch test section and is capable of operating at stagnation pressures ranging from about 16 to 90 psia. The tunnel can operate at temperatures from about 78 to 340 K. A 2000 KW variable speed motor drives a single stage fan which is the primary control for the test section Mach number. The tunnel is capable of running near Mach 1.

The tunnel is automatically controlled by a microcomputer to an accuracy of ± 0.2 K in temperature, ± 0.07 psia in pressure, ± 0.002 in Mach number and ± 0.04 million in Reynolds number based on model chord. (ref. 6) The tunnel test section has top and bottom flexible solid walls which can be set to any desired contour using stepper motor drives. A flexible wall adaptation system seeks low wall interference contour for any test model through an iterative search. (ref. 7) Each test section sidewall has a porous segment through which sidewall boundary-layer mass can be removed to control the boundary-layer at the wall and control flow separation at the airfoil model.

Boundary-layer removal system of the 0.3-m TCT:

Figure 1 shows a schematic for 0.3-m TCT sidewall boundary-layer control. The mass flows out of two porous segments of the test section sidewalls and is carried by two ducts through the plenum to two digitally controlled valves, DV1 and DV2. Each digital valve consists of 13 elements with a series of 14 sonic nozzles each having a throat area which is twice that of the previous element. The digital valve is expected to choke for very small pressure ratios, according to the manufacturer, and hence is expected to serve both as a mass flow controller, and measuring device. The discharge ends of the digital valves are connected. The mass flow out of the digital valves discharge end duct takes two paths. The first path is through valve BL1. During passive boundary-layer removal this valve is open to the atmosphere. The second path goes through an isolation valve and ends at the suction inlet to the compressor. Provision exists for spraying LN_2 into the compressor inlet duct. The LN_2 injection into the compressor inlet duct is through an 8 element digital valve which is intended to precisely control the mass flow of LN_2 from the LN_2 supply.

The centrifugal compressor is driven at about 21000 rpm by a variable speed 6 pole three phase 1000 HP water cooled alternating current induction motor. The compressor motor is supplied from a variable frequency generator system capable of generating 10-120 Hz three phase electrical supply with

constant voltage/frequency ratio. The compressor motor shaft is connected to the compressor through a 9.8:1 ratio gear box to step up the motor speed of about 2180 to about 21000 rpm. The compressor output branches into three paths. One path is to a tunnel reinjection valve which leads the compressor output flow back to the tunnel circuit. The second path is to a discharge valve, BL2, which discharges the compressor output to atmosphere. The third path leads the compressor outlet mass flow back to its inlet through surge valves, SV. The surge valves consist of a pair of pneumatically actuated valves driven by a process controller which keeps the compressor pressure ratio at or below 2.15. These surge valves open whenever the compressor pressure ratio exceeds the set value.

The sidewall boundary-layer mass flow removal electronic control system consists of a microprocessor based controller which drives the three digital valves, the compressor speed set point, and provides set point to surge controller according to a set of control laws. It also provides safety interlocking to prevent operation of the compressor until the flow path is complete. The system obtains data about the tunnel and the compressor system through a set of transducer signals which measure the inlet and outlet pressures of the digital valves, pipe temperature, tunnel total pressure, tunnel static pressure, tunnel gas temperature and the compressor motor speed. The mass flow through the digital valves, DV1 and DV2, are estimated in the controller based on the inlet pressure, inlet temperature and the valve area. In this algorithm, the flow is assumed to be choked and the valve C_D is used for mass flow estimation. The test section mass flow is also estimated based on tunnel flow conditions and nominal test section area. The estimated mass flow through the digital valves and the test section are displayed on the controller.

Passive mode of boundary-layer mass flow removal:

In the passive mode of boundary-layer mass flow removal, the compressor isolation valve and the reinjection valve are closed and the discharge valve, BL1, is open to the atmosphere. The compressor does not function in this mode. During normal operation the tunnel static pressure is higher than atmospheric pressure. The controller adjusts the digital valve area automatically to realize discharge of the desired mass flow from the sidewalls to the atmosphere. The desired mass flow is commanded on the controller either in mass dimensions or in percentage of the test section mass flow. The flow controller estimates the mass flow removal based on choked flow assumptions. This mode of operation of the system has been performing satisfactorily. (ref. 2)

Active mode of boundary-layer mass flow removal:

In the active mode of operation the discharge valves BL1 and BL2 are fully closed and the compressor

isolation valve and the reinjection valve are fully open. The compressor and the microprocessor based controller performs the following functions.

i) The compressor motor speed is run up to the maximum speed of about 2180 rpm for temperatures greater than 227 K or to a speed $145\sqrt{T}$ for lower temperatures.

ii) LN_2 is sprayed into the compressor inlet duct to keep the compressor discharge temperature at the same temperature as the tunnel total temperature.

iii) The pressure ratio across the compressor is measured. If the pressure ratio exceeds a preset value, the surge valves are opened to keep the compressor safely below a set pressure ratio. The pressure ratio schedule is:

$$R = 2.15 \qquad \text{for } T \leq 227 \text{ K}$$
$$R = \left(1+\frac{55.7}{T}\right)^{3.5} \qquad \text{for } T > 227 \text{ K}$$

iv) The digital valves, DV1 and DV2 areas are varied automatically to realize the desired mass flow set on the controller.

These functions are performed once every second. The controller monitors all the valve positions, and commands the digital valves through binary commands. The compressor speed control is through an on-off set of relays which drive the rheostat of a variable frequency generator and adjusts the compressor motor speed. The operators front panel controls include mass flow set points, mode selection for the controller and the valve positions.

ANALYSIS OF THE COMPRESSOR SYSTEM

Figure 1 shows a schematic of the existing 0.3-m TCT boundary-layer control. The compressor inlet flow is taken from the test section sidewalls just ahead of the airfoil station. The compressor discharges into the tunnel diffuser close to the LN_2 injection point. Since the compressor inlet and outlet pressures are determined by the tunnel circuit pressure, an analysis of the tunnel pressure profile at the points of interface with the compressor is necessary for an understanding of its performance.

Tunnel circuit pressure profile:

Figure 2 illustrates the contraction and the diffuser of a typical cryogenic tunnel. The flow in the contraction and the diffuser can be expressed by isentropic relations as follows (γ=1.4):

test section mass flow, $\dot{m}_t = K \frac{P_t}{\sqrt{T}} A_t \frac{M}{(1+ 0.2\ M^2)^3} = K \frac{P_d}{\sqrt{T}} A_d \frac{M_d}{(1+ 0.2\ M_d^2)^3}$ (1)

static pressure in the test section, $P_s = \frac{P_t}{(1+ 0.2\ M^2)^{3.5}}$ (2)

static pressure in the diffuser, $P_{sd} = \frac{P_d}{(1+ 0.2\ M_d^2)^{3.5}}$ (3)

If the mass flow removed $\dot{m}_{bl}(<< \dot{m}_t)$ from the test section is to be reinjected back in at the diffuser, the compressor must be capable of generating a pressure ratio in excess of the P_{sd}/P_s. Ignoring the small change of mass flow in the test section due to the diversion of a small fraction of the flow we have:

static pressure ratio, $\frac{P_{sd}}{P_s} = \frac{P_d}{P_t} \frac{(1+ 0.2\ M^2)^{3.5}}{(1+ 0.2\ M_d^2)^{3.5}}$ (4)

flow Mach number ratio can be found from the following expression,

$$\frac{M}{M_d} \frac{(1+ 0.2\ M_d^2)^3}{(1+ 0.2\ M^2)^3} = \frac{P_d\ A_d}{P_t\ A_t} \tag{5}$$

The total pressure ratio is a function of the tunnel loss coefficient for the section concerned, model blockage, and flexible wall shape. The local Mach number ratio is a function of the area ratio between the test section and the diffuser. Since the tunnel area A_d at the reinjection point of the diffuser is larger than the test section area A_t, the Mach number M_d is always lower than M, and the static pressure ratio P_{sd}/P_s of equation (4) is always greater than 1 for all Mach numbers. The tunnel pressure ratio between the test section and reinjection point can be obtained by solving equations (4) and (5). The pressure ratio is independent of the tunnel temperature and tunnel pressure. Since the pressure loss ratio P_t/P_d is related to the Mach number alone under isentropic conditions:

then, $$\frac{P_{sd}}{P_s} = \left(\frac{P_t}{P_d}\right)^{0.167} \left(\frac{A_t M}{A_d M_d}\right)^{1.167} \tag{6}$$

Using the 0.3-m TCT geometrical data for the area ratio A_d/A_t of 1.92 in equation (5) and approximating the total pressure ratios as unity we have:

$$\frac{P_{sd}}{P_s} = \left(\frac{1+ 0.2\ M^2}{1+ 0.054\ M^2}\right)^{3.5} \tag{7}$$

This expression is approximate and provides the nature of the pressure ratio needed by the compressor to create the necessary boundary-layer removal mass flow.

Flow analysis:

The compressor input is from two test section wall suction ducts. A positive mass flow through the ducts and the digital valves creates a pressure loss in the line and hence the compressor inlet pressure is lower than the test section wall static pressure. This pressure loss is a function of the mass flow and can be expressed as:

$$\Delta P = k_1 \dot{m}_{bl}^2 \frac{T}{P_s} \tag{8}$$

This identity can be derived from the continuity equation and state equation as follows. Pressure loss can also be expressed as:

$$\Delta P \propto \tfrac{1}{2}\rho v^2$$

where $\dot{m} = \rho v A$ and $\rho = \frac{P}{kT}$

then $$\Delta P \propto \tfrac{1}{2}\rho v^2 = \tfrac{1}{2}\rho \frac{\dot{m}^2}{\rho^2 A^2} = \frac{k \dot{m}^2 T}{2 P A^2}$$

Hence the compressor inlet and outlet pressures are:

$$P_{in} = P_s - k_1 \dot{m}^2_{bl} \frac{T}{P_s} \tag{9}$$

and

$$P_{out} = P_{in} R$$

The compressor mass flow can be expressed as a function of the test section mass flow from equation (1) in percent and equation (9) simplified as:

$$P_{in} = P_s [1 - k_2 \alpha^2 M^2 (1 + 0.2 M^2)] \tag{10}$$

where α is the percentile mass flow through the compressor normalized to the test section mass flow. For positive compressor mass flow $P_{in}R > P_d$ assuming no line losses in the discharge line:

then $$P_s [1 - k_2 \alpha^2 M^2 (1 + 0.2 M^2)] R > P_d \tag{11}$$

Equation (7) and (11) together can be used to generate the approximate solution to find the compressor pressure ratio needed for α percent mass flow removal from the test section and reinjection.

When $P_{in}R < P_d$ there is inadequate pressure ratio and the compressor discharge pressure P_{out} is less than the diffuser pressure P_d, reverse flow will occur with mass flow moving from the diffuser back to the test section.

The compressor-tunnel interface behavior can be predicted to yield active boundary-layer removal system performance. To do so, the compressor pressure ratio should be expressed as a function of compressor motor speed. Based on experimental data, the pressure ratio approximation is:

$$R = 1 + 1.317 \times 10^{-6} \left(\frac{N}{\sqrt{T}}\right)^{2.75} \qquad (12)$$

By treating equation (11) as an equality and using equation (12) and (7) in equation (11), the relationship between test section Mach number and the mass flow ratio α can be generated for various normalized compressor motor speeds. The constant k_2 in equation (10) and (11) has been estimated as 0.244 for each leg of the sidewall flow, based on experimental studies. This predicted system performance is shown in figure 3. It illustrates two features. First, with increasing Mach number, the mass flow that can be removed decreases asymptotically. Second, the figure illustrates the possibility of using compressor speed control for controlling mass flow removal rate. The figure also illustrates the possibility of reverse flow from the diffuser back into the test section when the compressor pressure ratio is low.

Compressor performance tests:

The 0.3-m TCT and compressor system have been tested together to evaluate the performance of the boundary-layer removal system as a part of the tunnel. For these test additional instrumentation was installed to measure the pressures around the compressor circuit. Instead of operating the compressor motor at a single constant speed of 2180 rpm, the compressor motor speed was varied to adjust the compressor mass flow. As the tunnel Mach number changes, the compressor pressure ratio required to prevent reverse flow also changes. The performance of the system was monitored both on the microprocessor based controller and by recording the pressures around the circuit.

Mass flow calibration:

The microprocessor based mass flow estimation and the display is based on the following equation.

$$\frac{1}{2}\dot{m}_{bl} = \frac{0.6992\ P_s}{\sqrt{T\ Z}}\ C_D\ A_v \qquad \text{(on each side)} \qquad (13)$$

This identity assumes that the digital valve is always choked. For choked conditions to exist in a nozzle, the output to input pressure ratio should exceed 0.528, according to isentropic relations. The digital valve manufacturer has suggested that the multiple nozzle type orifice systems in the digital valve shows choked behavior with pressure ratio of 0.85, for pressure drop as low as 15% loss. Under varying mass flow conditions, the pressure ratio across the digital valve varies from 1 to about 0.8. In most cases pressure loss across the digital valves during tunnel operation was less than 15%. This choked flow algorithm for mass flow estimation was found to be inadequate for small flows and gave erroneous estimates. This mass flow shown on the microprocessor based controller was always positive even when reverse flow situations existed in the system.

A mass flow algorithm which uses the measured pressure drop across the digital valves is more suitable for the sidewall boundary-layer removal system. The following identity can provide the true mass flow, based on measurement of the pressure drop across the digital valve.

$$\dot{m}_{bl} = C_{D1}\, A_v \sqrt{\frac{P_{in}}{T}\,\Delta P} \tag{14}$$

where C_{D1}=2.90 for the digital valve, A_v is normalized to 1 when full open, P and T refer to valve inlet states and ΔP is the pressure loss. This mass flow indicator can identify the reverse mass flow conditions, which is an essential requirement in the sidewall boundary-layer system.

Temperature control:

The compressor operation results in a temperature rise in the mass flow through the compressor. This temperature rise is a function of the compressor pressure ratio and can be expressed, based on isentropic relations as:

$$\Delta T = T\,\frac{(R^{(\frac{\gamma-1}{\gamma})}-1)}{R^{(\frac{\gamma-1}{\gamma})}} \tag{15}$$

At a maximum mass flow of about 8 kg/s through the compressor, and with a maximum power of about 400 KW, the estimated temperature rise is about 50 K. The microprocessor based control system can inject LN_2 into the compressor inlet duct, and has a proportional integral derivative (PID) algorithms to keep the compressor outlet temperature the same as the tunnel temperature.

The automatic temperature control system was not functioning during performance tests. This was due to engineering problems such as valve malfunction, two phase flow in the digital valve supply line

due to thermal leakage, and control law inadequacies. Hence, the option of letting the tunnel temperature control system handle this extra heating has been tried, since a gas temperature control loop already exists in the tunnel control system. The tunnel temperature control law could adjust for the extra heat energy from the compressor and still hold the tunnel gas temperature to within 0.1 to 0.2 K.

Performance tests:

The boundary-layer compressor tests were made with full open digital valves using compressor motor speeds varying from 700 to 2100 rpm in a variable speed mode. The temperature control of the compressor inlet through the boundary-layer system microprocessor was bypassed by shutting off the LN_2 supply. The tunnel and sidewall boundary-layer removal system tests were made at two temperatures of 150 and 240 K with tunnel total pressure being varied from 16 to 75 psia. In each case, the test section Mach number was varied from 0.3 to 0.8. At each tunnel condition, the boundary-layer compressor system could provide positive mass flow removal varying from near zero to the maximum by proper manual adjustment of compressor motor speed. The compressor circuit pressures, compressor motor speed, and the digital valve pressure loss were recorded and analyzed to evaluate the line pressure losses, the compressor pressure ratios, the tunnel pressure ratios, mass flows, and normalized compressor motor speed for each tunnel condition.

Discussion of experimental results:

The boundary-layer control compressor performance over the tunnel operating envelope is presented in the form of pressure ratio vs compressor motor speed in figure 4. This figure shows a typical compressor performance characteristic, with pressure ratio reaching a maximum of about 2.46 at a normalized compressor motor speed of 171. In the figure the compressor speed is normalized to the square root of temperature, and hence data from different temperatures regress into one typical pattern. The pressure ratio variability at any given speed represents different mass flows through the compressor, as dictated by the tunnel flow Mach number variation.

The compressor performance is also presented as the boundary-layer control compressor map in figure 5. This figure shows the compressor pressure ratio as a function of mass flow rate. The pressure ratio varies from 1.00 to nearly 2.46. The mass flow varies from 1 to 7 kg/s. The pressure ratio-mass flow rate control is obtained by varying the compressor motor speed, which is normalized to account for the effect of temperature variation. The system performance has been tested at 240 and 150 K. The temperature normalized compressor motor speeds vary from about 73 to 171 in seven steps and a locus

for each speed is presented in the figure 5. At the low speed of 73, low pressure ratios of 1.2 and mass flows of about 1 kg/s is realized. At the high speed of 171, pressure ratios realized are near 2.46 and the mass flow is in the range 6 to 7 kg/s. The compressor performance covers an inlet pressure variation ranging from 10 to 45 psia. The map shows a classical shape typical of turbocompressors. Once the compressor motor speed data was normalized to account for the temperature effects, the compressor map is independent of the tunnel temperature.

The 0.3-m TCT and compressor interface characteristics are presented in figure 6. This figure provides the normalized mass flow removal rate from the test section boundary-layer as a function of the test section flow Mach number. The plot clearly shows the ability of the compressor to remove as much as 10% of the test section flow at low Mach numbers. At high Mach numbers, the ability of the system to remove mass flow drops to about 4%. The mass flow removal rate can be smoothly controlled by varying the compressor speed. The surge limit of the pressure ratio-mass flow have not been encountered at any operating point during the tunnel-compressor system interface.

The estimated mass flow removal capability, based on analytical modeling discussed in equations (6), (10) and (11), is shown in figure 3. It can be compared to the experimentally derived mass flow removal capability shown in figure 6. The characteristics show generally good agreement in quality and magnitudes of mass removal. Discrepancies between figure 3 and 6 at low mass flow removal can be attributed to the inadequacies of the analytical model. The analytical model does not take in to account injection and ejector action of mass injection and removal process. In addition the Mach number ratio model of equation (6) is simplified considerably. The trend in performance predicted by the simple analytical model in equation (11) has a reasonable good match with the experimental system performance. It generally confirms the model of the flow mechanics between tunnel and the compressor proposed by the analytical model.

A NEW APPROACH TO BOUNDARY-LAYER MASS FLOW REMOVAL CONTROL

Presently existing concept:

The existing sidewall boundary-layer removal system as shown in figure 1 has been configured based on the control concept that the compressor always runs at near maximum speed to maintain a pressure ratio of about 2.15. The mass flow through the compressor is controlled by two throttling digital valves which control the flow area. Since the compressor is likely to surge at high pressure ratios when low mass flows are involved, a surge prevention recirculation path has been incorporated. The compressor surge control system receives an estimated maximum pressure ratio from the controller.

The surge suppression system prevents compressor surge bypassing the flow through valve SV so as to increase the gross mass flow through the compressor. Since considerable heat may be generated in this recircultaion, it is proposed to have LN_2 injection at the compressor inlet. The presently used control concept has potentially many problems. Even for small mass flows, the compressor has to run at high speeds near 21000 rpm. This results in unnecessary power loss in the throttling valves and during surge conditions complicating the temperature control problem. The compressor operates very near the surge all the time, and unnecessarily burdens the surge control.

Proposed concept:

Based on the results of test on the existing sidewall boundary-layer system, the following is proposed as an alternative for operating and controlling the boundary-layer system.

A new simplified ducting scheme as illustrated in figure 7. Its features are as follows:

1. Use of two new venturi or orifice plate system to measure mass flow out of the tunnel accurately. The pressure drop across the device provides an unambiguous measure of the true mass flow in each leg of the sidewall ducts.

2. The compressor is run at different speeds using the variable speed motor drive. The compressor operating speed is chosen to create the required mass flow and hence the compressor induced heating is minimal. In this scheme the suction line valves are kept full open.

3. The tunnel temperature control system can adequately handle this extra heat generated by the compressor. Hence there is no need for a LN_2 based cooling system in the compressor duct. This reduces the complexity of the plumbing and insulation associated with the existing LN_2 valve and duct. It also reduces the control law burden on the microprocessor based controller.

4. A number of valves presently existing can be deleted, and the lines can be optimized for minimum pressure loss and maximum thermal efficiency.

5. The compressor always operates away from the surge line since its speed is kept at the minimum required. The onset of surge is easily identified by pressure ratio measurement and action can be taken to avoid reaching the surge condition.

In the proposed control scheme, the controller functions involve analog to digital conversion of signals

from the compressor motor speed sensor, from the venturi/orifice plate pressure drop and the tunnel states. The digital to analog function is for the compressor motor speed control command. The digital input/output functions consist of logic signals from valve status and commands to valve drives. The test section mass flow and boundary-layer removal mass flow are estimated based on equations (1) and (14). An inner speed control loop based on a proportional integral (PI) algorithm controls the compressor motor speed. In the manual mode the operator adjusts the compressor motor speed to realize the desired boundary-layer mass flow removal based on the display. In the automatic mode, an outer loop adjusts the compressor motor speed to realize the boundary-layer mass flow removal set point based on the error between the command and the measured mass flows. The safety interlocks include the compressor flow path continuity assessment based on valve status. A safety trip for surge consists of identifying onset of surge based on pressure ratio/mass flow and reducing the speed of the compressor motor.

These control laws can be easily realized on a general purpose microcomputer of the 16 bit class. The control law mechanization involves dominantly software solutions and minimal hardware reconfiguration. Choice of a commercial quality microcomputer reduces the software and hardware complexities associated with presently used custom built microprocessor based controller.

CONCLUSIONS

The performance of the active sidewall boundary-layer removal system for the 0.3-m TCT has been predicted analytically using a simple flow model. The basic features of the model have been confirmed experimentally, thereby gaining insight into the boundary-layer removal compressor and cryogenic tunnel interface performance for various tunnel operating conditions. The sidewall boundary-layer removal compressor system of 1988 at the 0.3-m TCT is capable of providing about 4% mass flow removal rate at high Mach number conditions of M=0.8. The mass flow/pressure ratio performance of the compressor is adequate for realizing the necessary mass removal requirements. However, the mass flow removal scheme presently existing has inherent control and measurement problems. The compressor is always run at high pressure ratios near surge requires extra cooling. Mass flow control is accomplished by throttling the inlet valves. The mass flow measurement scheme based on digital valve choked flow assumptions has been unsatisfactory for operation in the active mode of boundary-layer removal.

A new scheme based on variable speed control of the compressor has been demonstrated to provide smooth mass flow control. It is shown that the temperature control burden imposed by the boundary-layer removal compressor can be transferred to the tunnel temperature control as long as no surge

recirculation occurs. The scheme covers the whole envelope of tunnel operating conditions in pressure, temperature, and Mach number and uses minimum necessary energy in realizing the mass removal from sidewall. The control algorithms needed for the variable speed approach are very simple and safe. The scheme proposes use of independent mass flow measurement based on pressure drop across a venturi or an orifice plate.

REFERENCES

1. Bernard-Guelle, R. : Influence of Wind Tunnel Boundary-Layers on Two-Dimensional Transonic Tests. NASA TT F-17, 255, October 1976.

2. Murthy, A. V. ; Johnson, Charles B. ; Ray, Edward J. ; Lawing, Pierce L. ; and Thibodeaux, J. J. : Studies of Sidewall Boundary-Layer in the 0.3-Meter Transonic Cryogenic Tunnel With and Without Suction. NASA TP-2096, March 1983.

3. Balakrishna, S. : Effects of Boundary-Layer Treatment on Cryogenic Wind-Tunnel Controls. NASA CR 159372, August 1980.

4. Johnson, Charles B. ; Murthy, A.V. ; and Ray, Edward J. : A Description of the Active and Passive Sidewall Boundary-Layer Removal Systems of the 0.3-Meter Transonic Cryogenic Tunnel. NASA TM 87764, November 1986.

5. Kilgore, Robert A. : Design Features and Operational Characteristics of the Langley 0.3-Meter Transonic Cryogenic Tunnel. NASA TN D-8304, December 1976.

6. Balakrishna, S. ; and Kilgore, W. Allen : Microcomputer Based Controller for the Langley 0.3-Meter Transonic Cryogenic Tunnel. NASA CR 181808, March 1989.

7. Wolf, Stephen W.D. : The Design and Operational Development of Self-Streamlining Two-Dimensional Flexible Walled Test Sections. NASA CR 172328, March 1984.

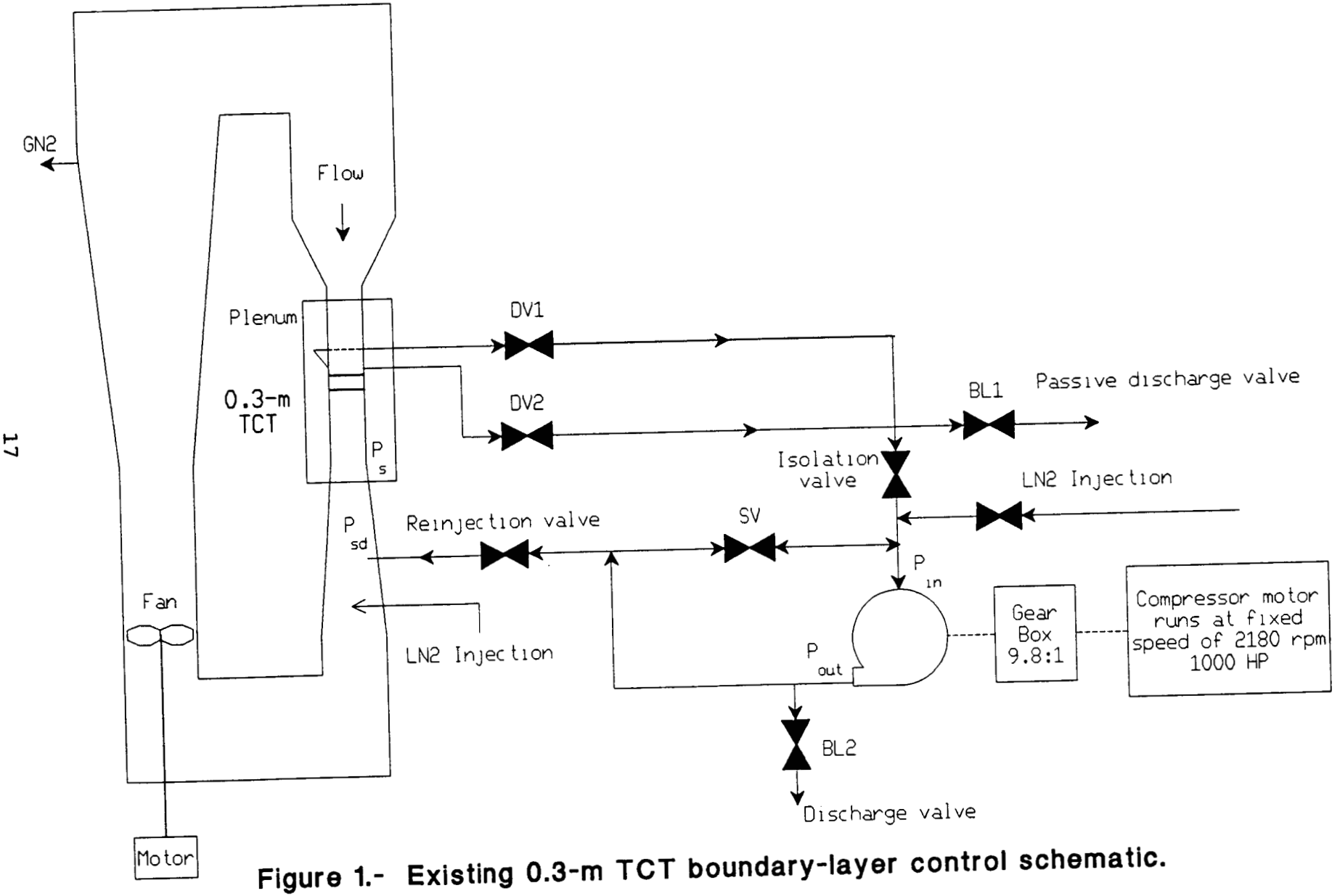

Figure 1.- Existing 0.3-m TCT boundary-layer control schematic.

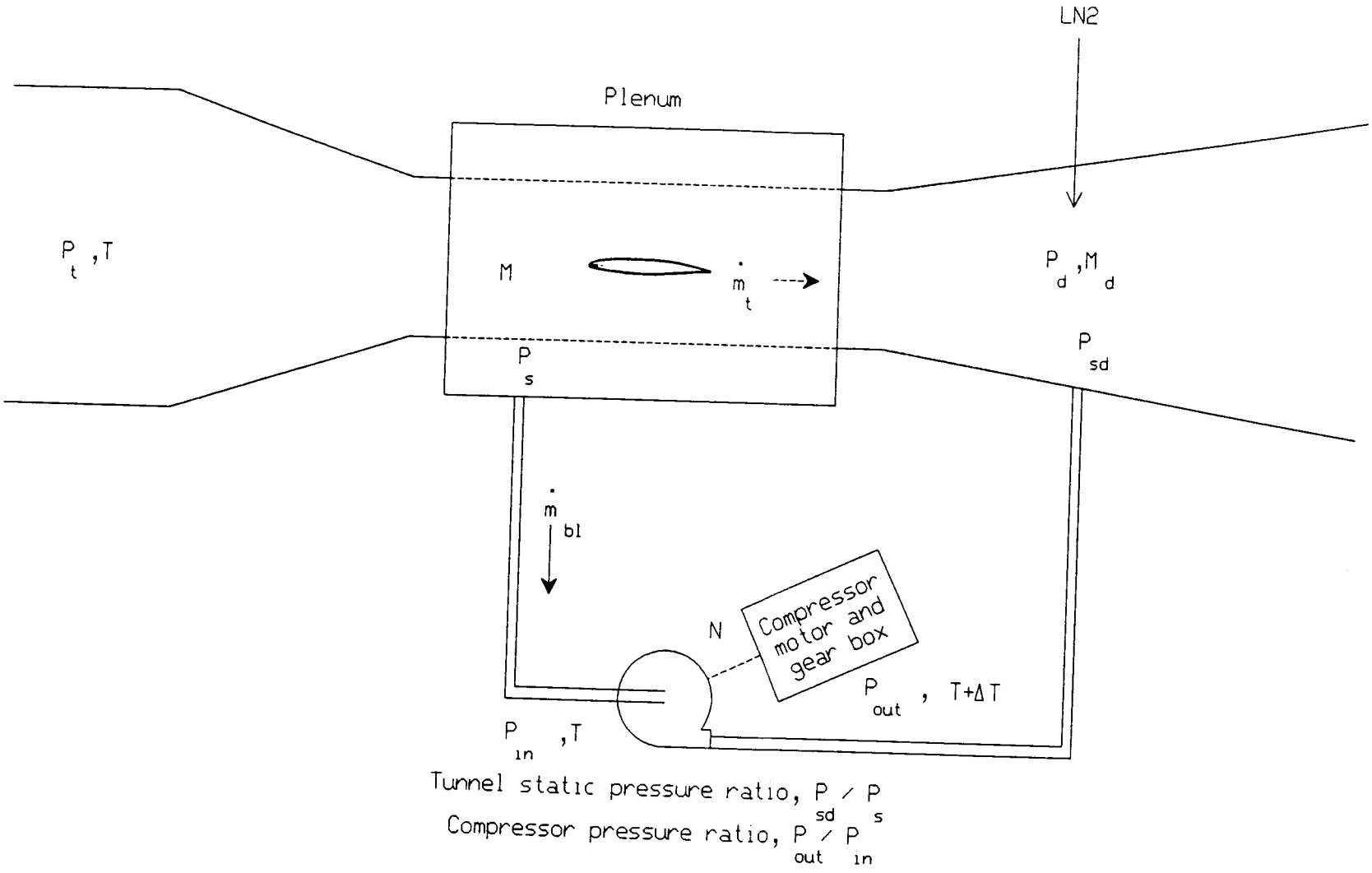

Figure 2.- Tunnel circuit and boundary-layer control compressor interface schematic.

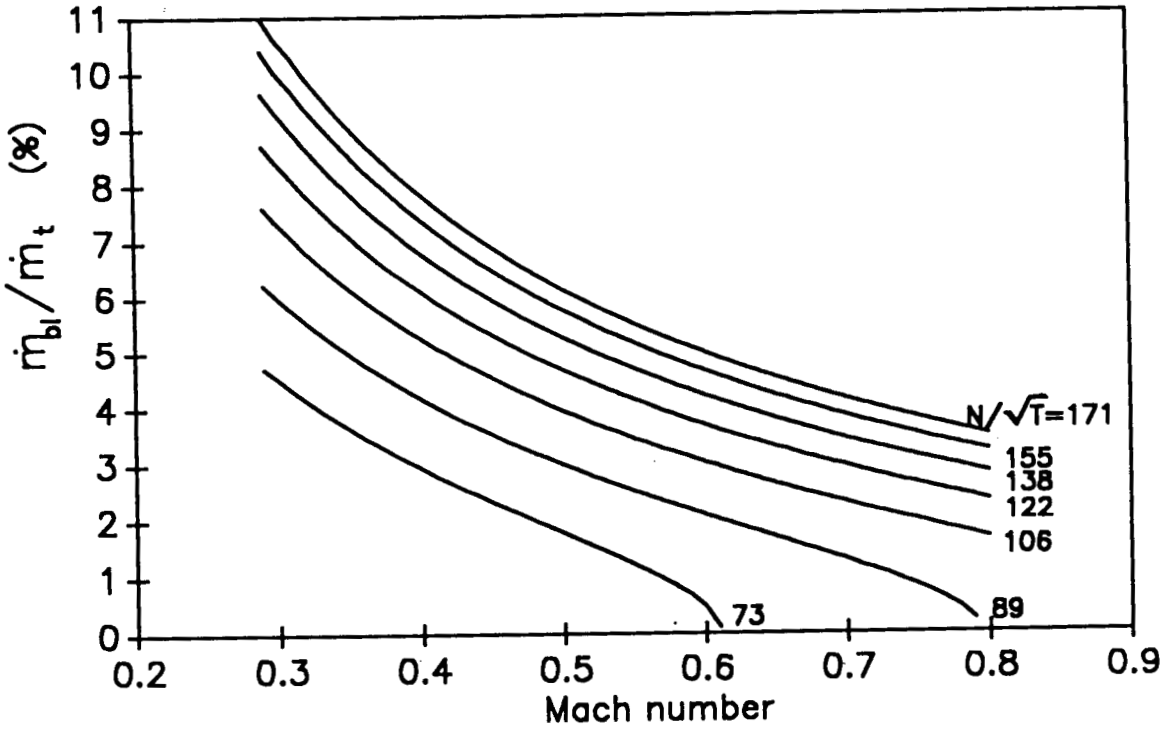

Figure 3.– Estimated performance of active boundary–layer removal system.

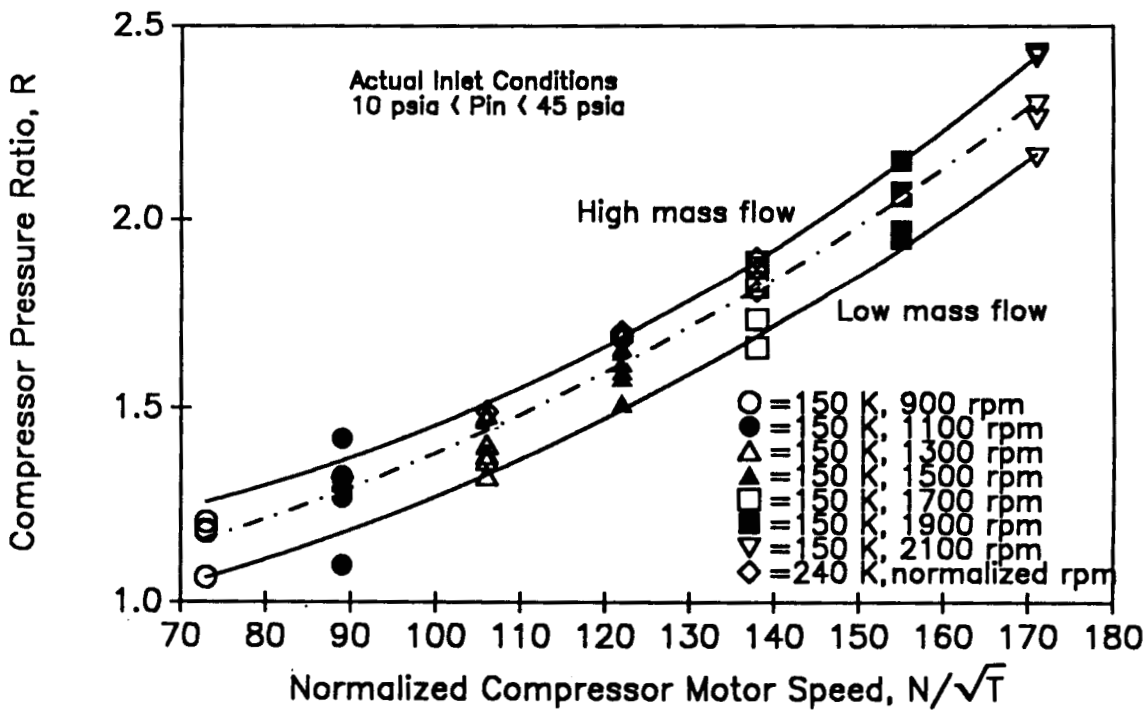

Figure 4.– 0.3–m TCT boundary–layer control compressor performance.

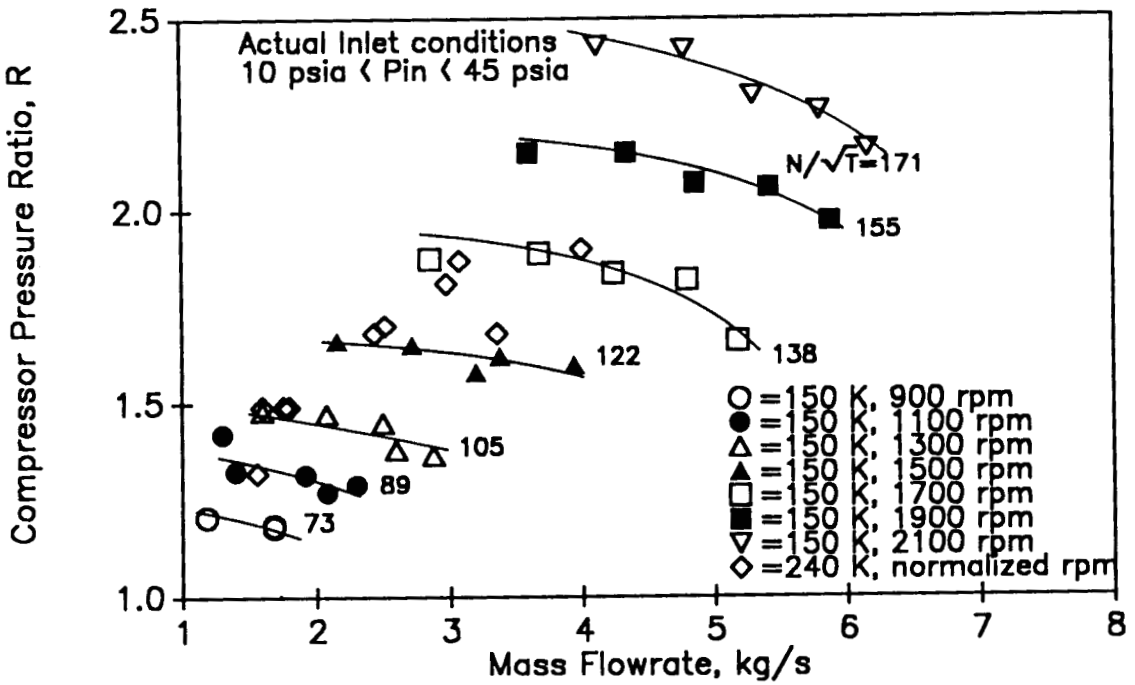

Figure 5.– 0.3–m TCT boundary–layer control compressor map.

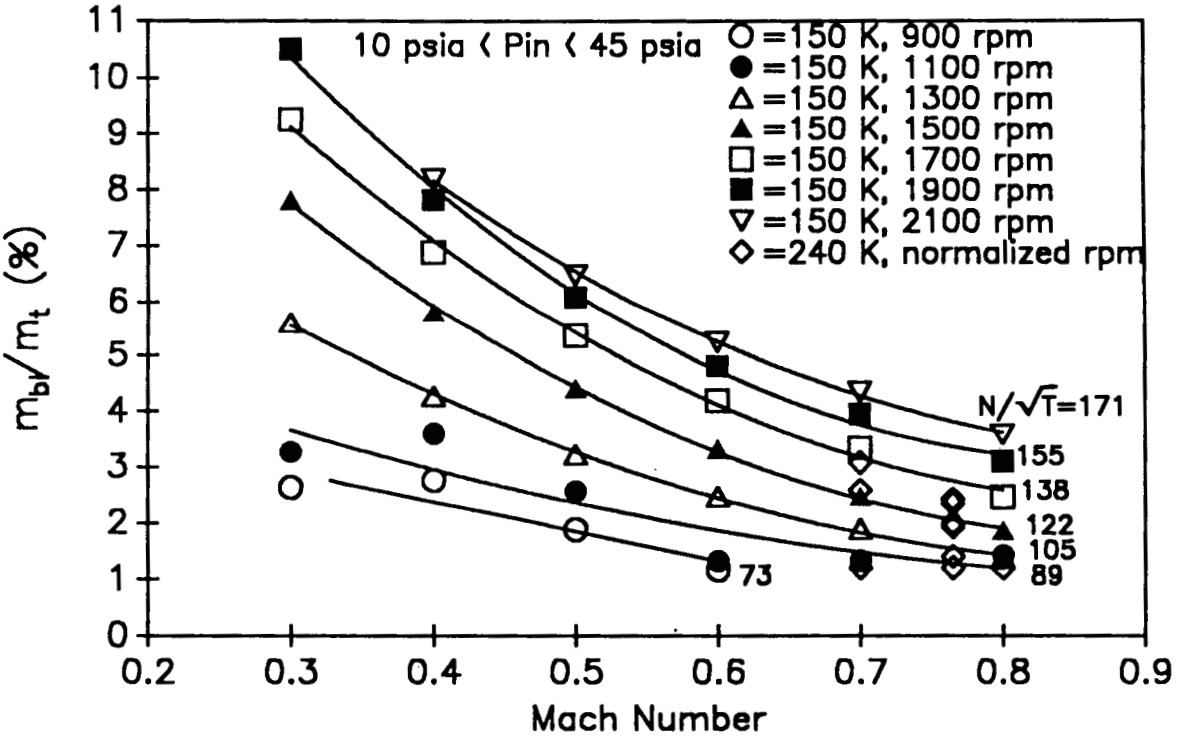

Figure 6.– Performance of 0.3–m TCT active boundary–layer removal system.

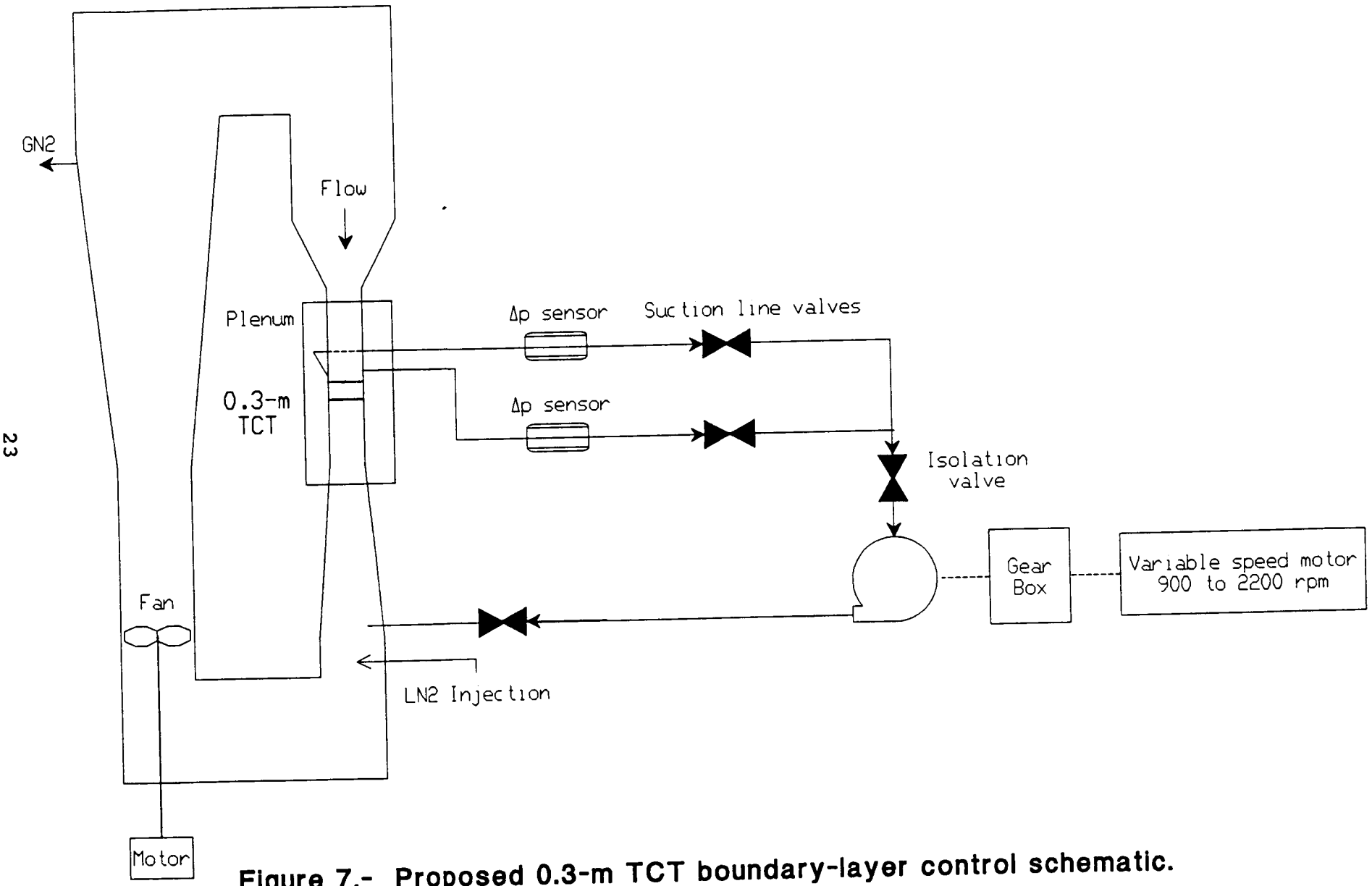

Figure 7.- Proposed 0.3-m TCT boundary-layer control schematic.

NASA National Aeronautics and Space Administration

Report Documentation Page

1. Report No.	2. Government Accession No.	3. Recipient's Catalog No.
NASA CR-181793		

4. Title and Subtitle	5. Report Date
Performance of the Active Sidewall Boundary-Layer Removal System for the Langley 0.3-Meter Transonic Cryogenic Tunnel	February 1989
	6. Performing Organization Code

7. Author(s)	8. Performing Organization Report No.
S. Balakrishna, W. A. Kilgore, and A. V. Murthy	
	10. Work Unit No. 505-61-01-09

9. Performing Organization Name and Address	11. Contract or Grant No.
Vigyan Research Associates, Inc. 30 Research Drive Hampton, VA 23665-1325	NAS1-17919
	13. Type of Report and Period Covered
12. Sponsoring Agency Name and Address	Contractor Report
National Aeronautics and Space Administration Langley Research Center Hampton, VA 23665-5225	14. Sponsoring Agency Code

15. Supplementary Notes

Langley Technical Monitor: Edward J. Ray

16. Abstract A performance evaluation of an active sidewall boundary-layer removal system for the Langley 0.3-m Transonic Cryogenic Tunnel (TCT) was evaluated in 1988. This system uses a compressor and two throttling digital valves to control the boundary-layer mass flow removal from the tunnel. The compressor operates near the maximum pressure ratio for all conditions. The system uses a surge prevention and flow recirculation scheme. A microprocessor based controller is used to provide the necessary mass flow and compressor pressure ratio control. Initial tests on the system indicated problems in realizing smooth mass flow control while running the compressor at high speed and high pressure ratios. An alternate method has been conceived to realize boundary-layer mass flow control which avoids the recirculation of the compressor mass flow and operation near the compressor surge point. This scheme is based on varying the speed of the compressor for a sufficient pressure ratio to provide needed mass flow removal. The system has a mass flow removal capability of about 10% of test section flow at M = 0.3 and 4% at M = 0.8. The system performance has been evaluated in the form of the compressor map, and compressor tunnel interface characteristics covering most of the 0.3-m TCT operational envelope. A simple analytical model which describes the compressor-tunnel interface flow mechanics has been proposed and validated.

17. Key Words (Suggested by Author(s))	18. Distribution Statement
Boundary-layer removal Cryogenic Tunnel	Unclassified - Unlimited Subject Category: 09

19. Security Classif. (of this report)	20. Security Classif. (of this page)	21. No. of pages	22. Price
Unclassified	Unclassified	24	A03

NASA FORM 1626 OCT 86